Quantum Electronics **45** (8) 691 – 696 (2015) ©2015 Kvantovaya Elektronika and Turpion Ltd

LASERS

PACS numbers: 42.55.Lt; 42.60.By; 42.60.Lh
DOI: 10.1070/QE2015v045n08ABEH015658

High-power, highly stable KrF laser with a 4-kHz pulse repetition rate

V.M. Borisov, A.V. El'tsov, O.B. Khristoforov

Abstract. **An electric-discharge KrF laser (248 nm) with an average output power of 300 W is developed and studied. A number of new design features are related to the use of a laser chamber based on an Al_2O_3 ceramic tube. A high power and pulse repetition rate are achieved by using a volume discharge with lateral preionisation by the UV radiation of a creeping discharge in the form of a homogeneous plasma sheet on the surface of a plane sapphire plate. Various generators for pumping the laser are studied. The maximum laser efficiency is 3.1 %, the maximum laser energy is 160 mJ pulse^{-1}, and the pulse duration at half maximum is 7.5 ns. In the case of long-term operation at a pulse repetition rate of 4 kHz and an output power of 300 W, high stability of laser output energy ($\sigma \leqslant 0.7$ %) is achieved using an all-solid-state pump system.**

Keywords: *excimer laser, KrF, preionisation, creeping discharge, ceramic laser chamber, C – C scheme, LC inverter, solid state pump system, high pulse repetition rate.*

1. Introduction

For more than 30 years, excimer lasers remain the most powerful sources of narrow-band radiation in the UV spectral region. Electric-discharge KrF lasers are distinguished among them by a unique combination of such characteristics as low radiation wavelength, high (for this class of lasers) efficiency (about 3%), high output energy (up to 1 J pulse^{-1}) and high average output power (~300 W and higher) [1, 2].

Because of this, electric-discharge KrF lasers find wide application in various technological processes. In particular, these lasers are used for 3D microprocessing of materials; formation of Bragg gratings on optical fibres, which operate as mirrors at the entrance and exit of waveguides [3]; production of second-generation high-temperature superconductor tapes [4]; laser annealing [5] and modification of materials, including photovoltaics [6, 7]; and irradiation of biological materials at a wavelength of 248 nm, which is close to the 265-nm wavelength corresponding to the maximum of the curve of relative bactericidal efficiency of UV radiation [8]. The optimal wavelengths of KrF and ArF lasers (i.e., the combination of a high energy of radiation photons with the possibility of using reliable quartz optics) stimulate the wide use of these lasers in large-scale lithographic manufacturing of integrated circuits [1]. For a long time, narrow-band KrF lasers with a relatively low (up to 10 mJ pulse^{-1}) energy and a high (4 kHz) pulse repetition rate served as a basis for this technology. At present, the laser projection lithography uses manly ArF lasers (193 nm), which make it possible to fabricate integrated circuits with a resolution of 45 nm and better [9, 10].

The active medium of high-power KrF lasers is excited by a repetitively pulsed high-pressure volume discharge in mixtures of Ne and Kr noble gases with molecular fluorine F_2 under the conditions of energy deposition into the discharge, which ensure high laser efficiency. This discharge is principally unstable, and its shape usually remains uniform for no more than several tens of nanoseconds. At the same time, the possibility of achieving desired laser characteristics is determined by a number of factors (whose interrelations are rather complicated), the main ones being the conditions of preionisation of the active volume, the regime of energy deposition into the discharge, the electrode system geometry and the characteristics of gas flow in this system [11 – 15]. The preionisation conditions include, first of all, a sufficiently high electron concentration created before the beginning of the main discharge development and a uniform electron distribution in the discharge volume.

In most high-power (~600 W) KrF lasers [2, 11, 15], UV preionisation was performed by multiple discrete spark discharges occurring at both sides of long metal electrodes, which provided a high concentration of initial electrons in the active volume of the laser. However, this lateral UV preionisation, due to the preioniser discreteness, does not ensure the main volume discharge uniformity, in particular, along the electrodes. In addition, the spark gaps of the preioniser are characterised by stronger electrode erosion. This limits the lifetime of the gas mixture of excimer lasers and reduces the laser operation stability in the long-term regime used in industrial applications.

To obtain intense uniform preionisation, we developed electrode systems of high-power excimer lasers with a highly efficient UV preioniser based on a completed creeping discharge (CD) in the form of a uniform plasma sheet on the surface of a sapphire plate positioned parallel to the laser electrodes [12, 13].

The long lifetimes of high-pressure excimer laser gas mixtures, which contain such extremely chemically active components as halogens, impose stringent requirements on the materials contacting with these mixtures and make it necessary to use a metal – ceramic laser chamber. We proposed to use a new chamber design based on a high-purity and high-quality Al_2O_3 ceramic tube, which was successfully implemented to create a high-power (500 W, 300 Hz) highly stable

V.M. Borisov, A.V. El'tsov, O.B. Khristoforov State Research Center of Russian Federation 'Troitsk Institute for Innovation and Fusion Research', ul. Pushkovykh 12, Troitsk, 142190 Moscow, Russia; e-mail: borisov@triniti.ru

Received 21 August 2014; revision received 30 October 2014
Kvantovaya Elektronika **45** (8) 691 – 696 (2015)
Translated by M.N. Basieva

compact wide-aperture (up to 55×30 mm) XeCl excimer laser with CD preionisation [16]. The operating lifetime of the gas mixture in this laser was $\sim 57 \times 10^6$ pulses at a stabilised average laser power of 450 W.

The aim of the present work is, using the developed approaches, to create a high-power highly stable excimer laser, in particular, a KrF laser, with a high (4 kHz) pulse repetition rate and a long gas mixture lifetime. To achieve a high stability of the high-power laser in the long-term regime, we study its operation with pump generators of various types.

2. Laser design

Figure 1 shows the transverse cross section of the laser chamber of a KrF excimer laser with a high pulse repetition rate. Similar to [16], we used the idea of creating a laser chamber based on an Al_2O_3 ceramic tube [17]. The laser chamber consists of a ceramic tube (*1*) (1100 mm long with an inner diameter of 360 mm) and end flanges (*2*) fastened together by bars (*3*). The end flanges with fastening bars form a metal frame, inside which the ceramic tube is placed. This frame is plated with metal sheets to suppress the electromagnetic noise from the functioning laser. From the bottom, the ceramic tube has fluoroplastic supports, so that the metal frame has no direct contact with the ceramic tube, which increases the laser chamber reliability.

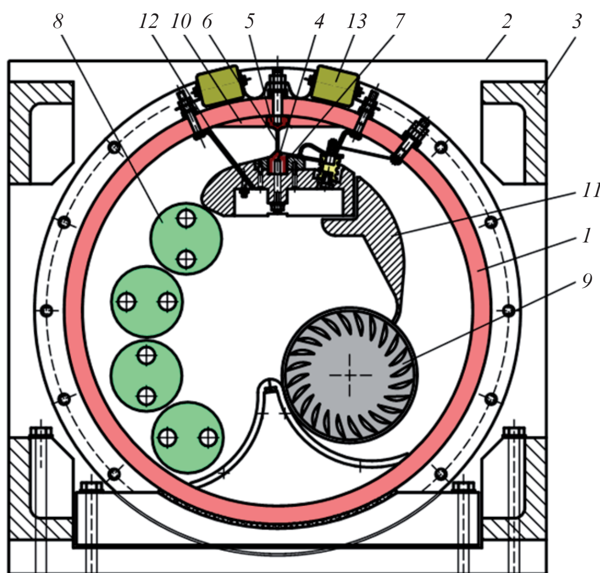

Figure 1. Design of the laser chamber of a high-power excimer laser with a high (up to 5 kHz) pulse repetition rate: (*1*) Al_2O_3 ceramic tube; (*2*) end flanges; (*3*) fastening bars; (*4*) grounded electrode; (*5*) high-voltage electrode; (*6*) discharge; (*7*) sapphire plate of the UV preioniser; (*8*) heat exchanger tubes; (*9*) cross-flow fan; (10) ceramic spoilers; (*11*) gas flow guides; (*12*) gas-transparent current-return leads; (*13*) ceramic capacitors.

Grounded and high-voltage electrodes (*4*) and (*5*) with a volume discharge gap (*6*) between them are located inside the laser chamber. The high-voltage electrode (*5*) is mounted directly on the ceramic tube. The other units of the laser chamber, namely, grounded electrode (*4*), preioniser (*7*) placed beside the grounded electrode, heat exchangers (*8*), cross-flow fan (*9*), ceramic spoilers (*10*) and gas flow guides (*11*), are supported only by the end flanges and do not touch the ceramic tube. The grounded electrode is connected to the power supply system through current-return wires (*12*), which are transparent for the gas flow and placed on both sides of electrodes. Outside the laser chamber, a set of ceramic capacitors (*13*) connected to electrodes (*4*) and (*5*) is distributed along the chamber. A pump generator connected to capacitors (*13*) impulsively charges them to a breakdown voltage, which initiates a gas discharge between the electrodes to excite the laser gas mixture. A typical optimal pressure of the gas mixture of the F_2–Kr–Ne laser was 2.6–3.1 atm.

It should be noted that the laser chamber design allows one to obtain lasing in both KrF and fluorides of other noble gases (ArF, XeF), as well as in F_2.

3. Pump generators

The laser characteristics depend to a large extent on the parameters of high-voltage pulses formed by a pump generator on the discharge gap of the laser. The ignition of the self-maintained preionised volume discharge, which pumps the laser active medium, occurs at the discharge voltage build-up stage. The higher the discharge-gap voltage (or the normalised electric field strength E/N) build-up rate, the more uniform the discharge and the higher its stability to, in particular, E/N spatial inhomogeneities formed by acoustic perturbations of the gas concentration N caused by preceding discharge pulses in the regime with a high pulse repetition rate f. At an optimal-high pump power density for the KrF laser ($\sim$2.5 MW cm^{-3}), the uniform volume discharge shape is retained for a characteristic time, which does not exceeds 60 ns [13]. All this imposes rigid requirements on the pump generators of excimer lasers, which must have high pulsed and average powers to generate high-current high-voltage short-duration pulses with a high repetition rate on the load. The schemes of pump generators used in the present work for investigation and optimisation of KrF laser parameters are shown in Fig. 2.

To decrease the discharge current duration, we used high-voltage high-current charge-transfer schemes, the simplest one being the C–C scheme presented in Fig. 2a. In this scheme, a storage capacitor C_0, which is charged (through a charging inductance L_c) from a high-voltage charger, is switched by a thyratron and impulsively discharges into a capacitor C_d low-inductively connected to the discharge gap. To achieve a high discharge-gap voltage build-up rate upon optimal pumping regimes in this scheme, the thyratron current amplitude usually exceeds admissible values, which leads to a decrease in the switch lifetime.

For all the schemes studied in this work (Fig. 2), the preionisation was performed by the UV radiation of a CD, which was automatically ignited upon charging capacitors C_{pr} ($C_{pr} \ll C_d$), which were connected to the laser electrodes via an auxiliary discharge gap of the completed CD formation system.

The most efficient pump generators for reliable long-term operation of repetitively pulsed lasers are the generators with a magnetic pulse compression system (Figs 2b, 2c) based on chains of series-connected circuits consisting of capacitors and nonlinear saturable inductors or magnetic switches MSs. The number of sequential circuits is selected to achieve the optimal high discharge-gap voltage amplitude and build-up rate at the nominal operating regimes of the switches.

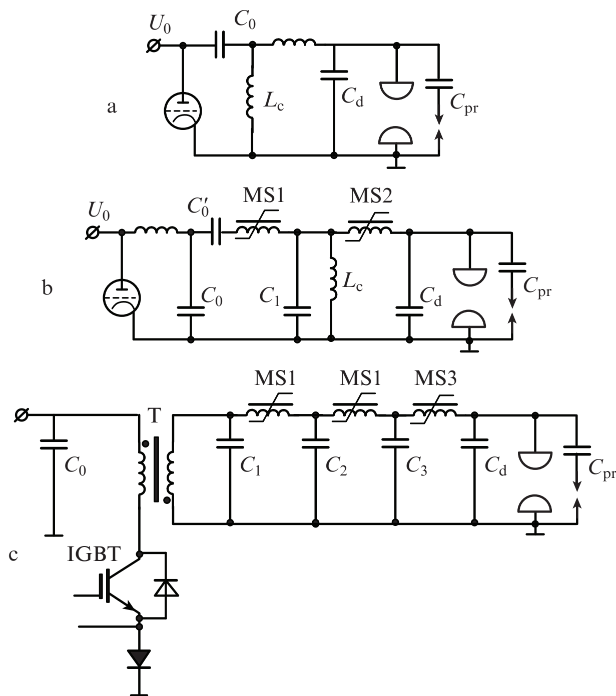

Figure 2. Schemes of the studied pump generators of a KrF laser: (a) *C–C* scheme; (b) *LC* inverter with two-stage pulse compression; and (c) all-solid-state scheme with IGBT switches and three-stage pulse compression.

The pump generator scheme shown in Fig. 2b is an *LC* inverter with two pulse-compression stages. This scheme made it possible to use as a switch a TGI 1000/25 thyratron with a current pulse duration of ~3 μs, which allowed the thyratron to operate for the entire nominal service life (no less than 10^9 pulses). Figure 3 shows typical oscillograms of the thyratron current, as well as of voltage pulses at the exit of the *LC* inverter in front of MS1, at the intermediate capacitor C_1 in front of MS2, and at the last-stage capacitor C_d connected to the laser electrodes. The discharge current amplitude was ~10 kA, and the duration of the first discharge current half-wave was ~30 ns. The first and second compression chains in the pump scheme included seven-turn (MS1) and two-turn (MS2) magnetic switches, which determined the total pump pulse compression coefficient (duration ratio of the switch and discharge currents) to be ~100.

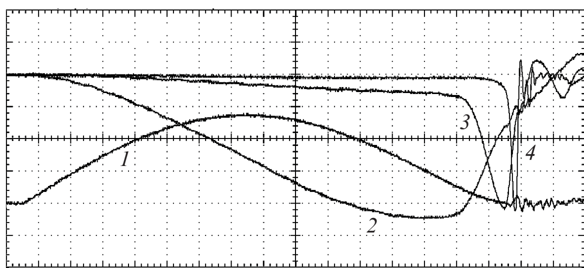

Figure 3. Oscillograms (*1*) of the thyratron current, as well as of the voltages (*2*) at the *LC* inverter exit; (*3*) at the intermediate capacitor C_1, and (*4*) at C_4, for a KrF laser with a pump generator based on an *LC* converter with two-stage pump pulse compression. The ordinate axis scale is 200 ns div^{-1}; the abscissa axis scales are 200 A div^{-1} and 5 kV div^{-1}.

As switches, which are the most important units of pumping generators, one currently widely uses high-power insulated-gate bipolar transistors (IGBTs), which have almost infinite service life and ensure a high stability of the parameters of voltage pulses [3, 18]. An all-solid-state generator scheme is shown in Fig. 2c. This pump generator with semiconductor switches (pulser) includes a step-up transformer T and is placed in a tank with transformer oil or other dielectric fluid, which ensured its cooling, reliable electrical insulation, suppression of electromagnetic noise and compactness of the laser design. The pump generator was supplied from a charger with a maximum output voltage of 2.2 kW and a power up to 20 kV, which provided resonance charging of the storage capacitor C_0.

4. Output laser characteristics

The laser was tested using electrodes 95 cm long with a 3-mm cone radius of the working part. The interelectrode gap was 22 mm for the systems shown in Figs 2a, 2b and 18 mm for the scheme in Fig. 2c, the discharge width being 3 mm and the length, 910 mm, which corresponded to the active volumes of 60 and 49 cm^3 for Figs 2a, 2b and Fig. 2c, respectively. This gas discharge gap geometry is typical for excimer lasers used as lithographic sources for industrial production of integrated circuits. For operation with high pulse repetition rates, a small discharge width is preferable since it simplifies the scheme of gas replacement in the discharge gap during intervals between discharge pulses. Another factor important for the choice of the discharge gap geometry for lithographic lasers is that the laser linewidth must be decreased to a value below 1 ps. For this purpose, one uses cavities with line narrowing modules. In this case, the laser beam size and, hence, the discharge width must be decreased to a value comparable with the effective size (3–4 mm) of the aperture of the line-narrowing module. As a rule, the discharge width of lithographic excimer lasers must be ~2 mm at an interelectrode gap of ~20 mm or smaller. A discharge width of 2 mm was used in an ArF laser.

At a high pulse repetition rate, the controlled velocity of interelectrode gas flow formed by the gas-circulation system was ~30 m s^{-1}. Below, the experimental data for all the schemes shown in Fig. 2 are given for the optimised capacities C_d = 9.5 nF and C_{pr} = 0.5 nF.

An advantage of preionisation by the UV radiation of a completed CD compared to the corona discharge preionisation, which is usually used, in particular, in lithographic lasers, consists in the possibility of controlling the energy deposition into the auxiliary CD within wide limits. The preionisation by a completed CD in the form of a uniform plasma sheet at a dielectric surface (sapphire plate) provides as high preionisation level as spark preionisation and is free of such its drawbacks as spatial inhomogeneity, which decreases the laser energy stability and efficiency at high pulse repetition rates, and severe erosion of spark electrodes, which decreases the gas mixture lifetime. The characteristic rate of ionisation by the UV radiation of a completed CD is ~0.5×10^{18} electron s^{-1} [19] at a pulse duration of ~30 ns. The preionisation processes in excimer lasers, which depend on electron attachment to the gas mixture components and on the voltage pulse applied to the electrodes, as well as the most efficient preionisation regimes in excimer lasers, are considered in [20].

The experimentally determined gas mixture composition optimal with respect to the average laser power was $F_2 : Kr : Ne = 3 : 70 : 2600$ mbar.

The MgF_2 windows of the laser chamber were inclined to the laser axis at the Brewster angle. The remote cavity was formed by a multi-layer mirror with a reflection coefficient exceeding 99 % at a wavelength of 248 nm and a plane-parallel CaF_2 plate (without coating).

Figure 4 presents the dependences of the laser efficiency η and energy W on the charging voltage U_0 for pump generators with a thyratron switch (Figs 2a, 2b) at the pulse repetition rate $f = 100$ Hz. Hereinafter, the efficiency is determined as the ratio of the laser energy to the electric energy stored in the storage capacitors C_0 for schemes in Figs 2a, 2c and C_0, C_0' for the scheme in Fig. 2b.

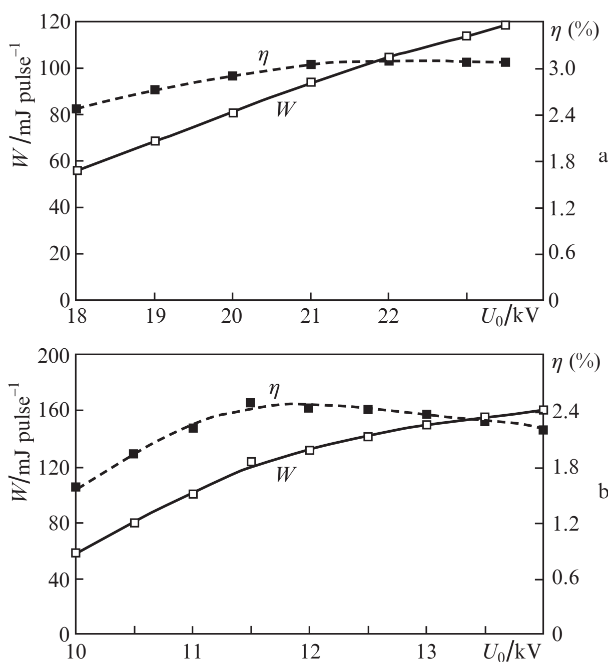

Figure 4. Dependences of the pulse energy W and efficiency η of a KrF laser on the charging voltage U_0 of a pump generator based on (a) a $C-C$ scheme and (b) an LC inverter.

In the $C-C$-scheme with the storage capacity $C_0 = 14$ nF, the maximum laser energy was 120 mJ pulse^{-1} and the maximum laser efficiency was 3.1 % (Fig. 4a).

In the scheme with an LC inverter (Fig. 2b), in which the storage capacities were $C_0 = C_0' = 35$ nF and the stored energy was variable by the charging voltage U_0 in a wider range than in the case of the $C-C$ scheme, the maximum power W reached 160 mJ pulse^{-1}. The maximum laser efficiency ($\eta \approx 2.5\%$) was lower than in the case of the $C-C$ scheme, which is mainly related to the presence of magnetic switches absorbing a noticeable part of the stored energy.

Laser efficiencies close to the maximum values ($\eta \approx 2.4\%$) were obtained for another scheme (Fig. 2c) with magnetic pump pulse compression, in which the stored energy was lower than for the scheme in Fig. 2b, the specific energy deposition into the discharge being 44 J L^{-1}. The characteristics of the laser with the pump scheme shown in Fig. 2b only slightly changed as the interelectrode gap h decreased from 22 to 18 mm, because of which we hereafter use for this scheme an

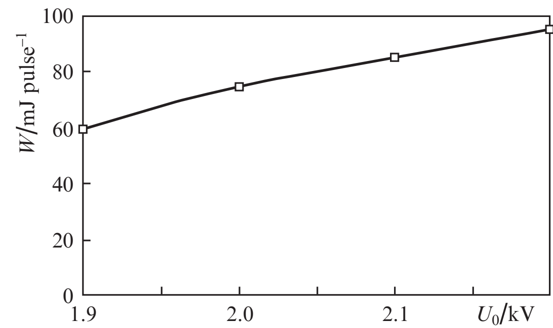

Figure 5. Dependences of the laser pulse energy W on the charging voltage U_0 in the case of a pump generator based on an all-solid-state scheme with semiconductor switches.

electrode system with $h = 18$ mm. From Fig. 5, one can see that the maximum laser energy of 96 J pulse^{-1} was limited by the maximum charging voltage $U_0 = 2.2$ kV.

For lasers with pump generators based on an LC inverter and an all-solid-state scheme, Fig. 6 presents the dependences of the average laser power P and the standard deviation of the output energy σ on the pulse repetition rate f.

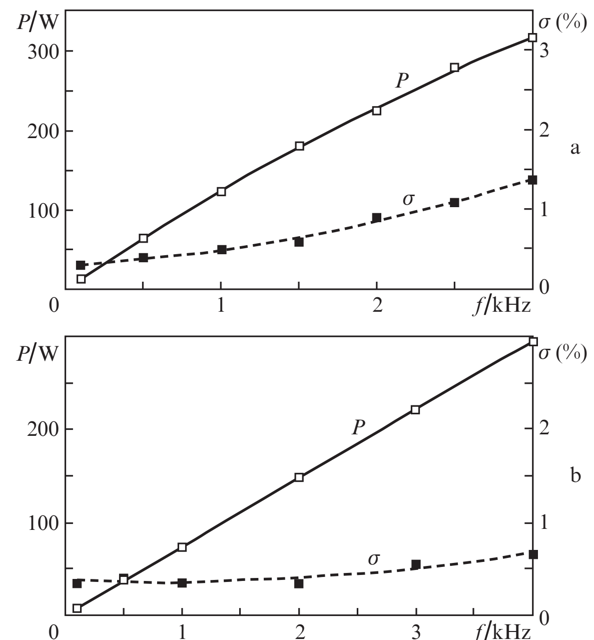

Figure 6. Dependences of the average laser power P and the standard deviation of the output energy σ on the pulse repetition rate of pump generators based on (a) an LC inverter and (b) an all-solid-state scheme with semiconductor switches.

From Fig. 6a, one can see that the average laser power of 315 W was obtained at $f = 3$ kHz using a pump generator with a thyratron switch designed according to the scheme in Fig. 2b. In this case, the relative laser energy instability σ monotonically increases with increasing f and reaches 1.4%. An increase in f above 3 kHz is accompanied by a sharp increase in the laser energy instability.

A higher laser pulse repetition rate and a higher laser energy stability were achieved with the use of an all-solid-state pump system with semiconductor switches (Fig. 6b).

The maximum average laser power achieved at $f = 4$ kHz was 295 W. Upon continuous operation for many hours with the pulse repetition rate $f = 4$ kHz, the parameter σ did not exceed 0.7%, which testifies to a high stability and reliability of the developed high-power excimer laser.

Figure 7 shows a series of laser pulse energies measured at $f = 4$ kHz, which demonstrates a high laser stability. A typical oscillogram of laser pulses with a duration of 7.5 ns at half width is shown in Fig. 8.

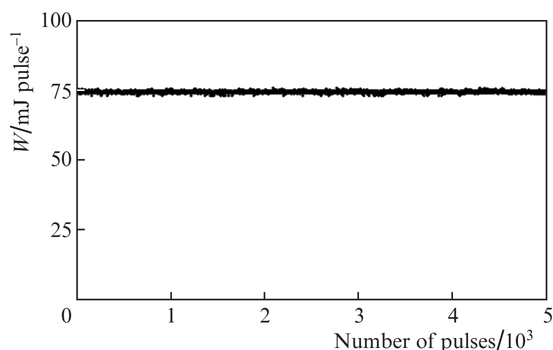

Figure 7. Series of laser pulse energies at the pulse repetition rate $f = 4$ kHz, which demonstrates a high laser stability ($\sigma = 0.7\%$).

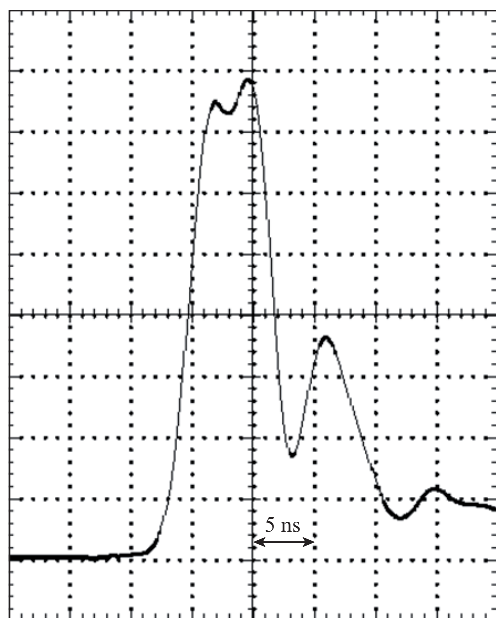

Figure 8. Laser pulse oscillogram.

For a plane-parallel cavity, the radiation divergence measured along two mutually perpendicular directions [along the smallest (θ_x) and largest (θ_y) dimensions of the laser beam] was $\theta_x \times \theta_y = 0.6 \times 1.4$ mrad, which corresponds to $6\theta_{dx} \times 80\theta_{dy}$, where $\theta_{di} = 2\lambda/D_i$ ($i = x, y$) is the diffraction divergence of a rectangular beam with the aperture $D_x \times D_y$ [21]. Despite the rather large beam divergence, the laser was successfully used for discharge initiation in high-power EUV light sources [22, 23], pulsed laser ablation for deposition of coatings [24], etc.

At the same time, for some applications it is desired to have radiation with better divergence. For this purposes, we developed and fabricated a series of optical schemes including a cylindrical unstable cavity, which, as we expect, will allow us to improve the divergence θ_y to $1.7\theta_{dy} \approx 0.03$ mrad. In addition, we fabricated a cylindrical mirror telescope and a lens telescope, both having a magnification $M = 8$. With the use of a telescope, we hope to increase the horizontal laser beam dimension to 24 mm and improve the horizontal divergence θ_x to 0.08 mrad. As a hole, using these optical systems, we expect to achieve the laser beam divergence $\theta_x \times \theta_y \approx 0.08 \times 0.03$ mrad.

5. Conclusions

The results of our investigations show that the proposed and developed approach to the creation of high-power excimer lasers with the use of a new type of a metal–ceramic laser chamber based on an Al_2O_3 ceramic tube allows one to achieve a high power (300 W) UV (248 nm) laser radiation with a high pulse repetition rate ($f = 4$ kHz). The use of the developed preionisation system based on a completed CD in the form of a uniform plasma sheet directed along the laser electrode simultaneously with the use of the all-solid-state pump generator with a magnetic pulse compression system allowed us to achieve highly stable ($\sigma = 0.6\%$) long-term operation of a KrF laser at $f = 4$ kHz.

References

1. Basting D., Pippert K., Stamm U. *Proc. SPIE Int. Soc. Opt. Eng.*, **4426**, 14 (2002).
2. Borisov V.M., Vinokhodov A.Yu., Vodchits V.A., Demin A.I., El'tsov A.V., Basting D., Stamm U., Voss F. *Kvantovaya Elektron.*, **25** (2), 126 (1998) [*Quantum Electron.*, **28** (2), 119 (1998)].
3. Basting D., Marowsky G. (Eds) *Excimer Laser Technology* (Berlin: Springer, 2005).
4. Ohmatsu K., Abiru K., Yamaguchi T., Shingai Y., Konishi M. *Techn. Rev.*, No. 73, 45 (2011).
5. Limanov A.B., Borisov V.M., Vinokhodov A.Yu., Demin A.I., El'tsov A.V., Kirukhin Yu.B., Khristoforov O.B. In: *Perspectives, Science and Technologies for Novel Silicon on Insulator Devices* (Dordrecht: Kluwer Academic Publisher, 2000) pp 55–61.
6. Tetsuya S., Taihei O., Norihiro T., Kota O., Mitsuhiro H., Daisuke N., Hiroshi I., Tanemasa A., Tatsuo O. *Appl. Phys. A*, **114** (2), 625 (2014).
7. Azumaa H., Takeuchia A., Itoa T., Fukushimaa H., Motohiroa T., Yamaguchib M. *Sol. Energy Mater. Sol. Cells*, **74** (1-4), 289 (2002).
8. Lawrence J., Waugh D.G. *Laser Surface Treatment of a Polymeric Biomaterial: Wettability Characteristics and Osteoblast Cell Response Modulation* (Philadelphia: Old City Publishing, 2013).
9. Brown D.J.W., O'Keeffe P., Fleurov V.B., et al. *Proc. SPIE Int. Soc. Opt. Eng.*, **6520**, 652020 (2007).
10. Asayama T., Sasaki Y., Nagashima T., Kurosu A., Hiroaki Tsushima, et al. *Proc. SPIE Int. Soc. Opt. Eng.*, **8683**, 86831G (2013), DOI:10.1117/12.2011404.
11. Borisov V.M., Vinokhodov A.Yu., Vodchits V.A., El'tsov A.V., Basting D., Stamm U., Voss F. *Kvantovaya Elektron.*, **25** (2), 131 (1998) [*Quantum Electron.*, **28** (2), 123 (1998)].
12. Borisov V.M., Demin A.I., Eltsov A.V., Khristoforov O.B., Kiryukhin Y.B., et al. *Proc. SPIE Int. Soc. Opt. Eng.*, **5137**, 241 (2003).
13. Borisov V.M., Khristoforov O.B. In: *Entsiklopediya nizkotemperaturnoi plasmy. Ser. B.* (Encyclopaedia of Low-Temperature Plasma. Ser. B) (Moscow: Fizmatlit, 2005) Vol. 11, Book 4, p. 503.

14. Andramanov A.V., Kabaev S.A., Lazhintsev B.V., Nor-Arevyan V.A., Pisetskaya A.V., Selemir V.D. *Kvantovaya Elektron*., **36** (2), 101 (2006) [*Quantum Electron*., **36** (2), 101 (2006)].
15. Borisov V.M., Vinokhodov A.Yu., Vodchits V.A., El'tsov A.V., Ivanov A.S. *Kvantovaya Elektron*., **30** (9), 783 (2000) [*Quantum Electron*., **30** (9), 783 (2000)].
16. Borisov V.M., Demin A.I., Khristoforov O.B. *Kvantovaya Elektron*., **45** (3), 200 (2015) [*Quantum Electron*., **45** (3), 200 (2015)].
17. Borisov V.M., Khristoforov O.B. European Patent EP1525646B1, published 23.12.2009.
18. Vartapetov S.K., Gryaznov O.V., Malashin M.V., Moshkunov S.I., Nebogatkin S.V., Khasaya R.R., Khomich V.Yu., Yamshchikov V.A. *Kvantovaya Elektron*., **39** (8), 714 (2009) [*Quantum Electron*., **39** (8), 714 (2009)].
19. Borisov V.M., Khristoforov O.B. In: *Entsiklopediya nizkotemperaturnoi plasmy. Vvodnyi tom II* (Encyclopaedia of Low-Temperature Plasma. Introductory Volume II) (Moscow: Nauka, 2000) Book II.
20. Borisov V.M., Demin A.I., El'tsov A.V., Novikov V.P., Khristoforov O.B. *Kvantovaya Elektron*., **26** (3), 204 (1999) [*Quantum Electron*., **29** (3), 204 (1999)].
21. Ready J.F., Farson D.F., Feeley T. (Eds) *LIA Handbook of Laser Materials Processing* (Berlin–Heidelberg–New York: Springer-Verlag, 2001).
22. Borisov V.M., Vinokhodov A.Yu., Ivanov A.S., Kiryukhin Yu.B., Mishchenko V.A., Prokof'ev A.V., Khristoforov O.B. *Kvantovaya Elektron*., **39** (10), 967 (2009) [*Quantum Electron*., **39** (10), 967 (2009)].
23. Borisov V.M., Borisova G.N., Vinokhodov A.Yu., Zakarov S.V., Ivanov A.S., Kiryukhin Yu.B., Mishchenko V.A., Prokof'ev A.V., Khristoforov O.B. *Kvantovaya Elektron*., **40** (8), 720 (2010) [*Quantum Electron*., **40** (8), 720 (2010)].
24. Borisov V.M., Kuz'menko V.A., Khristoforov O.B. *Inzh. Fiz*., **4**, 34 (2014).